Relating Topological Determinants of Complex Networks to Their Spectral Properties: Structural and Dynamical Effects

Claudio Castellano[1] and Romualdo Pastor-Satorras[2,*]

[1]*Istituto dei Sistemi Complessi (ISC-CNR), Via dei Taurini 19, I-00185 Roma, Italy*
[2]*Departament de Física, Universitat Politècnica de Catalunya, Campus Nord B4, 08034 Barcelona, Spain*

The largest eigenvalue of a network's adjacency matrix and its associated principal eigenvector are key elements for determining the topological structure and the properties of dynamical processes mediated by it. We present a physically grounded expression relating the value of the largest eigenvalue of a given network to the largest eigenvalue of two network subgraphs, considered as isolated: the hub with its immediate neighbors and the densely connected set of nodes with maximum K-core index. We validate this formula by showing that it predicts, with good accuracy, the largest eigenvalue of a large set of synthetic and real-world topologies. We also present evidence of the consequences of these findings for broad classes of dynamics taking place on the networks. As a by-product, we reveal that the spectral properties of heterogeneous networks built according to the linear preferential attachment model are qualitatively different from those of their static counterparts.

Subject Areas: Complex Systems, Statistical Physics

I. INTRODUCTION

The spectral properties of complex topologies [1] play a crucial role in our understanding of the structure and function of real networked systems. Various matrices can be constructed for any given network, their spectral properties accounting for different topological or functional features. Thus, for example, the Laplacian matrix is related to diffusive and random walk dynamics on networks [2], the modularity matrix plays a role in community identification on networks [3], and the nonbacktracking or Hashimoto matrix governs percolation [4]. Among all matrices associated with networks, the simplest and possibly most studied is the adjacency matrix A_{ij}, taking the value 1 whenever nodes i and j are connected, and zero otherwise. Particular interest in this case is placed on the study of the principal eigenvector $\{f_i\}$ (PEV), defined as the eigenvector of the adjacency matrix with the largest eigenvalue Λ_M (LEV). This interest is twofold. On the one hand, the PEV is one of the fundamental measures of node importance or centrality [5]. The centrality of a node can be defined based on the number of different vertices that can be reached from it, or the role it plays in connecting different parts of the network. From a more sociological point of view, a node is central if it is connected to other central nodes. From

this definition, we get the notion of eigenvector centrality of a node [6], which coincides with the corresponding component of the PEV. On the other hand, the LEV plays a pivotal role in the behavior of many dynamical systems on complex networks, such as epidemic spreading [7], synchronization of weakly coupled oscillators [8], weighted percolation on directed networks [9], models of genetic control [10], or the dynamics of excitable elements [11]. In these kinds of dynamical processes, the LEV is related, through different analytical techniques, to the critical point at which a transition between different phases takes place: In terms of some generic control parameter λ, a critical point λ_c is found to be, in general, inversely proportional to the LEV Λ_M.

The possibility of knowing the position of such transition points in terms of simple network topological properties is of great importance, as it allows us to predict the system's macroscopic behavior or optimize the network to control processes on it. This has triggered intense activity [12–15], particularly in the case of networks with heterogeneous topology, such as power-law distributed networks with a degree distribution of the form $P(q) \sim q^{-\gamma}$ [16]. Among these efforts, in their seminal work [17], Chung, Lu, and Vu (CLV) have rigorously proven, for a model with power-law degree distribution, that the LEV can be expressed in terms of the maximum degree q_{max} present in the network and the first two moments of the degree distribution. This is a remarkable achievement, as it allows us to make predictions in the analysis of dynamics on networks.

Here, we show that while the CLV theory provides, in some cases, an excellent approximation to the LEV, especially in the case of random uncorrelated networks, it can fail considerably in other cases. In order to provide

*Corresponding author.
romualdo.pastor@upc.edu

better estimates, we reinterpret the CLV result in terms of the competition among different subgraphs in the networks. This insight leads to the formulation of a modified form of the CLV theory that captures the behavior of the LEV more generally, including the case of real correlated networks, and asymptotically reduces to the CLV form in the case of random uncorrelated networks. We show that our generalized expression perfectly predicts the LEV for linear preferential attachment (LPA) growing networks (for which the original CLV form fails) and provides an excellent approximation for the LEV of real-world networks. Finally, we show that our modified expression reliably predicts the critical point of dynamical processes on a large set of synthetic and real-world networks, with no exception.

The paper is organized as follows: In Sec. II, we review the original expression for the largest eigenvalue from Ref. [17] and show how it can lead to large errors in real correlated networks. In Sec. III, we present physical arguments substantiating a new generalized expression for the largest eigenvalue, whose validity is checked against a large set of real networks. In Sec. IV, we discuss in detail the case of growing linear preferential attachment networks, which turn out to be a remarkable benchmark for the plausibility of our new generalized expression. We discuss the effects of our prediction in the estimation of the critical point in epidemics and synchronization dynamics in Sec. V. Finally, we present our conclusions and future avenues of work in Sec. VI. Several appendixes provide details and additional information.

II. CHUNG-LU-VU FORMULA FOR THE LARGEST EIGENVALUE

In Ref. [17], the authors consider a class of network models with a given expected degree distribution. In other words, starting from a predefined degree distribution $P(q)$, one generates expected degrees $\tilde{q}_i$ for each node, drawn from $P(q)$, and creates an actual network by joining every pair of nodes i and j with probability $\tilde{q}_i \tilde{q}_j / \sum_r \tilde{q}_r$. The resulting network has a degree distribution with the same functional form as the imposed $P(q)$ and lacks degree correlations since the condition $\tilde{q}_i^2 < \sum_r \tilde{q}_r$ is imposed in the construction [17,18]. This algorithm is a variation of the classical configuration model [14], cast in terms of a hidden variables model [19]. For this model network, and any arbitrary degree distribution, the authors in Ref. [17] rigorously prove that the largest eigenvalue of the corresponding adjacency matrix takes the form (see also Ref. [20])

$$\Lambda_M = \begin{cases} a_1 \sqrt{q_{\max}} & \text{if } \sqrt{q_{\max}} > \frac{\langle q^2 \rangle}{\langle q \rangle} \ln^2(N) \\ a_2 \frac{\langle q^2 \rangle}{\langle q \rangle} & \text{if } \frac{\langle q^2 \rangle}{\langle q \rangle} > \sqrt{q_{\max}} \ln(N), \end{cases} \quad (1)$$

where N is the network size, $q_{\max}$ is the maximum degree in the networks, and a_i are constants of order 1. In the case of scale-free networks, the maximum degree is a growing function of N, which, for uncorrelated networks [21], takes

the value $q_{\max} \sim N^{1/2}$ for $\gamma \leq 3$ and $q_{\max} \sim N^{1/(\gamma-1)}$ for $\gamma > 3$ [18]. The algebraic increase of $q_{\max}$ allows us to disregard the logarithmic terms in Eq. (1) in the limit of infinite-size networks, leading to the simpler expression [22]

$$\Lambda_M \approx \max\{\sqrt{q_{\max}}, \langle q^2 \rangle / \langle q \rangle\}, \quad (2)$$

valid for any value of γ. For power-law distributed networks, the second moment of the degree distribution scales as $\langle q^2 \rangle \sim q_{\max}^{3-\gamma}$ for $\gamma \leq 3$ and $\langle q^2 \rangle \sim$ const for $\gamma > 3$. Combining this result with the expression for the maximum degree, we can write the more explicit result

$$\Lambda_M \approx \begin{cases} \sqrt{q_{\max}} & \text{if } \gamma > 5/2 \\ \frac{\langle q^2 \rangle}{\langle q \rangle} & \text{if } \gamma < 5/2. \end{cases} \quad (3)$$

It is important to remark that while Eq. (2) holds for asymptotically large networks, its applicability to networks of finite (yet huge) size should not be taken for granted. The exact Eq. (1) does not provide predictions for a wide (size-dependent) range of values of the ratio $\langle q^2 \rangle / [\langle q \rangle \sqrt{q_{\max}}]$. As shown in Appendix A, uncorrelated power-law distributed networks fall within this range for the span of network sizes usually considered in computer simulations, so Eq. (1) does not provide predictions about any uncorrelated power-law networks that can be numerically simulated. Nevertheless, Eq. (2), which is a nonrigorous generalization of the exact Eq. (1), turns out to be very accurate for random uncorrelated static networks even of small size. Indeed, in Fig. 1(a), we present a scatter plot of Λ_M computed using the power iteration method [23] in random uncorrelated power-law networks generated with the uncorrelated configuration model (UCM) [24], for different values of the degree exponent γ and network size N, as a function of the numerically estimated value of $\max\{\sqrt{q_{\max}}, \langle q^2 \rangle / \langle q \rangle\}$. The agreement with Eq. (2) (in the following denoted
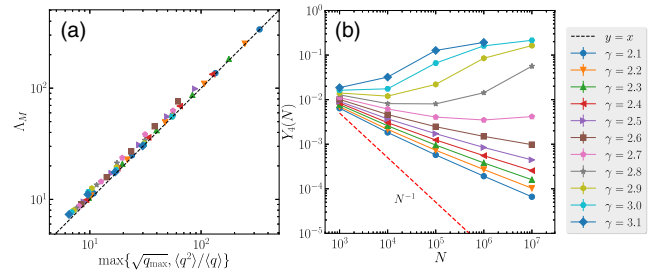

FIG. 1. (a) Largest eigenvalue Λ_M as a function of $\max\{\sqrt{q_{\max}}, \langle q^2 \rangle / \langle q \rangle\}$ in uncorrelated power-law UCM networks with different degree exponent γ and network size N. (b) Inverse participation ratio $Y_4(N)$ as a function of N in uncorrelated power-law UCM networks with different degree exponent γ. Each point in both graphs corresponds to an average over 100 independent network realizations. Error bars are smaller than symbol sizes. Networks have a minimum degree $m = 3$.
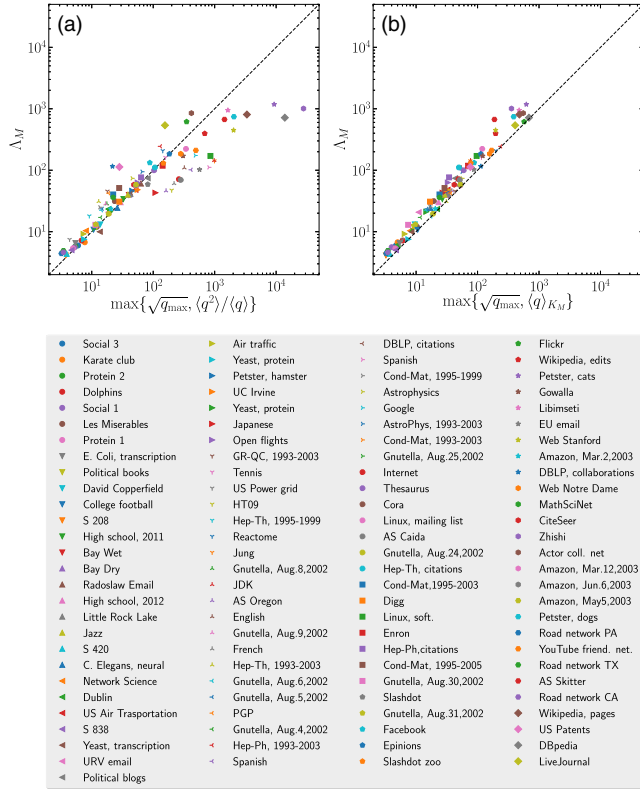
FIG. 2. (a) Largest eigenvalue Λ_M as a function of $\max\{\sqrt{q_{max}}, \langle q^2\rangle/\langle q\rangle\}$ computed for 109 different real-world networks. (b) Largest eigenvalue Λ_M as a function of $\max\{\sqrt{q_{max}}, \langle q\rangle_{K_M}\}$ computed for the same real-world networks. Networks are ordered by increasing network size.

as CLV theory) is almost perfect, with only very small deviations for the smallest network sizes.

In order to test the generality of CLV theory beyond uncorrelated networks, we have also considered a large set of 109 real-world networks (the same as considered in Ref. [25]; see this reference for network details), of widely different origin, size, and topological features. In Fig. 2(a), we plot the LEV of these networks as a function of the numerically estimated quantity $\max\{\sqrt{q_{max}}, \langle q^2\rangle/\langle q\rangle\}$. The result is quite clear: While in some cases the CLV prediction works well, in others it provides an overestimation of the actual value of the LEV that can be larger than one order of magnitude. This discrepancy is particularly strong in the case of the Zhishi, DBpedia, and Petster, cats networks, but it is considerable in a large number of other cases.

III. GENERALIZED FORMULA FOR THE LARGEST EIGENVALUE

We can understand the origin of the violations of the CLV formula observed in Fig. 2(a) and provide an improved version by reconsidering the observations made in Refs. [26,27]. In these works, it is shown that the two

types of scaling of the LEV in the CLV formula for uncorrelated networks (either proportional to $\langle q^2\rangle/\langle q\rangle$ or to $\sqrt{q_{max}}$) are the manifestation of the two alternative ways in which the PEV can become localized in the network (see Appendix B). For $\gamma > 5/2$, the PEV is localized around the node with the largest degree in the network (the hub), and the scaling of Λ_M is given by $\sqrt{q_{max}}$; for $\gamma < 5/2$, on the other hand, the PEV becomes localized (in the sense discussed in Ref. [27]) on the core of nodes of maximum index K_M in the K-core decomposition of the network [28,29] (see Appendix C); the associated LEV is then given by $\langle q^2\rangle/\langle q\rangle$. This picture is confirmed in Fig. 1(b), where we study the localization of the PEV, of components $\{f_i\}$ assumed to be normalized as $\sum_i f_i^2 = 1$, in random uncorrelated networks. The analysis is performed by plotting the inverse participation ratio [27,30,31] $Y_4(N)$ as a function of the network size (see Appendix B). As we can check, for $\gamma > 5/2$, $Y_4(N)$ goes to a constant for $N \to \infty$, indicating localization in a finite set of nodes that coincide with the hub and its immediate neighbors. On the other hand, for $\gamma < 5/2$, the inverse participation ratio decreases algebraically with network size, with an exponent α smaller than 1, indicating localization in a subextensive set of nodes, which coincide with the maximum K-core [27]. Additional evidence is presented in Appendix D.

This observation can be interpreted in the following way: The actual value of the LEV in the whole network is the result of the competition among two different subgraphs. The node with the largest degree q_{max} (the hub) and its immediate neighbors form a star graph, which, in isolation, has a largest eigenvalue given by $\Lambda_M^{(h)} = \sqrt{q_{max}}$. On the other hand, the maximum K-core, of index K_M, is a densely interconnected, essentially degree-homogeneous subgraph [26]. As such, its largest eigenvalue is given by its internal average degree, $\Lambda_M^{(K_M)} \approx \langle q\rangle_{K_M}$. In the case of uncorrelated networks, this average degree is well approximated by $\langle q^2\rangle/\langle q\rangle$ [29]. These two subgraphs, and their respective largest eigenvalues, $\Lambda_M^{(h)}$ and $\Lambda_M^{(K_M)}$, compete in order to set the scaling of the LEV of the whole network: The global LEV coincides with the subgraph LEV that is larger.

We hypothesize that for generic networks, including correlated ones, the same competition sets the overall LEV value. The largest eigenvalue of the star graph centered around the hub is trivially still equal to $\sqrt{q_{max}}$. What changes in general topologies, and, in particular, in correlated networks, is the expression of the largest eigenvalue associated with the maximum K-core. One can realistically assume that the maximum K-core is, in general, degree homogeneous (see the heterogeneity parameter of the maximum K-core or real-world networks in Table 1 in Ref. [32], which is, except in one case, smaller than 1). What cannot be taken for granted, in general, is the identification between $\langle q\rangle_{K_M}$ and $\langle q^2\rangle/\langle q\rangle$. We thus conjecture that the LEV in generic networks can be expressed as

$$\Lambda_M \approx \max\{\sqrt{q_{\max}}, \langle q \rangle_{K_M}\}. \qquad (4)$$

Equation (4) is the central result of our paper. Note that Eq. (4) is valid in full generality for any network if the approximation sign $\approx$ is replaced by $\geq$, as Rayleigh's inequality guarantees that the largest eigenvalue of any subgraph is a lower bound for the LEV of the whole network [1]. Our conjecture here is that this lower bound is also a very good approximation, in the sense that Λ_M differs at most from the lower bound by a factor of the order of a few units.

Note that Eq. (4) includes Eq. (2) as a particular case when $\langle q \rangle_{K_M} \approx \langle q^2 \rangle / \langle q \rangle$, which is true in uncorrelated networks [29]. Moreover, Eq. (4) is in agreement with some known exact results for specific classes of networks. A simple example is provided by random q-regular graphs. They have LEV equal to q, which is also the average degree of the max K-core, and it is larger than $\sqrt{q_{\max}} = \sqrt{q}$. A less trivial example is given by random trees grown according to the linear preferential attachment rule (see Sec. IV). Bhamidi *et al.* [33] show that, in this case, the LEV is exactly $\sqrt{q_{\max}}$, the value predicted by Eq. (4) since, by construction, $\langle q \rangle_{K_M} = 2$. Another related exact result concerns the $G(N, p)$ (Erdös-Rényi) random network, for which Krivelevich and Sudakov [34] have proven that $\Lambda_M = (1 + o(1)) \max\{\sqrt{q_{\max}}, Np\}$, where the term $o(1)$ tends to zero as the $\max\{\sqrt{q_{\max}}, Np\}$ tends to infinity and Np is the average degree $\langle q \rangle$. According to Ref. [29], for Erdös-Rényi networks, the highest K-core is linear with the average degree, $K_M \sim 0.78 \langle q \rangle$, and the mean degree of the K-core depends weakly on the core and $\langle q \rangle_K \simeq \langle q \rangle$. Hence, our Eq. (4) agrees with the result of Krivelevich and Sudakov for Erdös-Rényi networks.

In Fig. 2(b), we check the validity of the proposed generalized scaling for the LEV in the case of the 109 real-world networks considered above. Comparing with Fig. 2(a), the generalized formula provides a much better overall fit to the real value of the LEV than the original CLV expression and therefore represents a better prediction for the behavior of this quantity. The overall improvement of our prediction versus the original CLV one can be established by comparing the absolute relative errors, with respect to actual measured LEVs, of the values predicted by Eqs. (2) and (4), respectively. The average relative error for Eq. (2) is 1.213, with standard deviation 3.285, and a maximum of 26.686; for Eq. (4), the average is 0.282, with standard deviation 0.154 and maximum 0.719. We conclude that Eq. (4) provides an excellent approximation for the LEV value of an extremely broad variety of networks. Additional evidence of its predictive power is presented in the next section.

Despite this vast generality, there are, however, particular classes of networks for which the lower bound is not tight and Eq. (4) is not a good approximation. These cases are examined in our discussion, Sec. VI.

IV. CASE OF LINEAR PREFERENTIAL ATTACHMENT NETWORKS

Growing network models provide a particularly interesting test bed for the conjecture presented above. We focus, in particular, on LPA networks [16,35], generated starting from a fully connected nucleus of $m + 1$ nodes and adding at every time step a new node with m new edges connected to m old nodes. For the vertex introduced at time t, each of its emanating edges is connected to an existing vertex s, introduced at time $s < t$, with probability

$$\Pi_s(t) = \frac{q_s(t) + a}{\sum_j [q_j(t) + a]}, \qquad (5)$$

where $q_s(t)$ is the degree, measured at time t, of the node introduced at time s. The factor a takes into account the possible initial attractiveness of each node, prior to receiving any connection. Large LPA networks are characterized by a power-law degree distribution $P(k) \sim k^{-\gamma}$, with a degree exponent $\gamma = 3 + (a/m)$ [36] and average degree $\langle q \rangle = 2m$. It is thus possible to tune the degree exponent in the range $2 < \gamma < \infty$ by changing the attractiveness parameter in the range $-m < a < \infty$. The power-law form extends up to the maximum degree $q_{\max}$ that depends on N as $q_{\max} \sim N^{1/(\gamma-1)}$ for all values of γ. LPA networks are further characterized by the presence of degree correlations [37]: The average degree of the nearest neighbors of nodes of degree q, $\bar{q}_{nn}(q)$ [38] is of the form $\bar{q}_{nn}(q) \sim q^{-3+\gamma}$ for $\gamma < 3$, and $\bar{q}_{nn}(q) \sim \ln q$ for $\gamma > 3$ [36]. See Appendix E for a practical implementation of this model.

By their very construction, LPA networks lack a non-trivial K-core structure since the iterative procedure to determine K shells for $K > m$ removes all nodes by exactly reversing the growth process. Therefore, in LPA networks, all nodes belong to the same $K = m$ shell, where m is the minimum degree in the network. We thus have $\langle q \rangle_{K_M} = \langle q \rangle = 2m \ll \sqrt{q_{\max}}$ even for modest values of N, and according to our generalized prediction, the LEV should be approximately $\sqrt{q_{\max}}$ for all values of γ, in stark opposition to the original CLV formula, which still predicts, in Eq. (3), different expressions for $\gamma < 5/2$ and $\gamma > 5/2$. This scaling, $\Lambda_M \sim \sqrt{q_{\max}}$, has been exactly demonstrated for the case $\gamma = 3$, corresponding to the so-called Barabasi-Albert model [16] in Ref. [39]. Here, we extend this form for all values of γ in LPA networks.

In Fig. 3(a), we plot the largest eigenvalue obtained in LPA networks with different sizes and degree exponent γ, as a function of $\sqrt{q_{\max}}$. As we can observe, after a short preasymptotic regime for small network sizes (small $q_{\max}$), Λ_M grows as $\sqrt{q_{\max}}$ for all values of γ, independently of the factor $\langle q^2 \rangle / \langle q \rangle$. Interestingly, for all values of γ, the LEV falls onto the same universal curve, asymptotically approaching $\sqrt{q_{\max}}$, which indicates that this functional form is, moreover, independent of degree correlations,
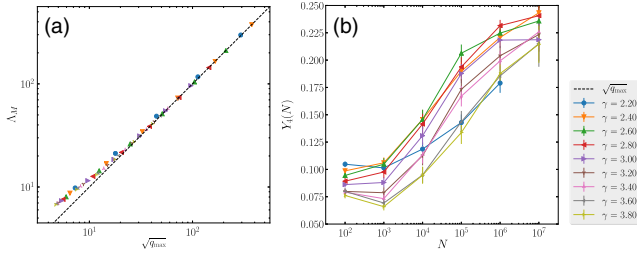
FIG. 3.   (a) Largest eigenvalue Λ_M as a function of $\sqrt{q_{max}}$ in LPA networks with different degree exponent γ. (b) Inverse participation ratio $Y_4(N)$ as a function of N in LPA networks with different degree exponent γ. Each point in both graphs corresponds to an average over 100 independent network realizations. Error bars are smaller than symbol sizes.

which change continuously with γ in LPA networks [36]. We conclude that, in perfect agreement with our conjecture, the spectral properties of LPA networks are ruled only by the hub. Additionally, this implies that the PEV is localized around the hub. This fact is verified in Fig. 3(b), where we plot the inverse participation ratio $Y_4(N)$ as a function of N. In Fig. 3(b), we see clearly that $Y_4(N)$ goes to a constant for $N \to \infty$, for any degree exponent γ and for sufficiently large N, indicating that PEV always becomes localized on a set of nodes of finite size (not increasing with N): the hub and its immediate neighbors. Further evidence about the localization is provided in Appendix F.

In LPA networks, the lack of a K-core structure is a fragile property since reshuffling connections while preserving the degree of each node [40] may induce some K-core structure. However, this emerging K-core structure is not able to restore the scaling predicted by Eq. (2) (see Appendix G). As Fig. 4(a) shows, reshuffling does not alter the overall behavior, apart from minimal changes: The LEV still scales asymptotically as $\sqrt{q_{max}}$ for any γ, while the PEV is still asymptotically localized around the hub, as the inverse participation ratio tending to a constant for large network sizes shows [see Fig. 4(b)].
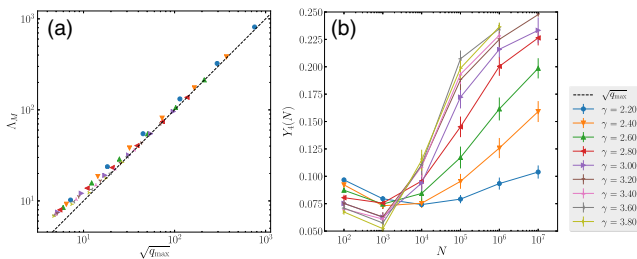
V. CONSEQUENCES FOR DYNAMICS ON NETWORKS

The spectral properties of the adjacency matrix determine the behavior of many dynamical processes mediated by topologically complex contact patterns [8–10,22,41]. Here, we show the consequences of the topological properties uncovered above for two highly relevant types of dynamics.

A. Epidemic spreading

The susceptible-infected-susceptible (SIS) model is one of the simplest and most fundamental models for epidemic spreading [42] (see Appendix H for details), showing an epidemic threshold λ_c separating a regime where epidemics rapidly become extinct from a regime where they affect a finite fraction of the system. The dependence of this threshold on the network topology is well approximated by the so-called quenched mean-field theory (QMF) (see Appendix H), predicting it to be equal to the inverse of the LEV,

$$\lambda_c = \frac{1}{\Lambda_M}. \tag{6}$$

Inserting into this expression the LEV scaling form given by Eq. (2) in the case of random uncorrelated static networks, we see that the threshold always vanishes on power-law distributed networks in the thermodynamic limit, with different scalings depending on the value of γ [22]. For $\gamma < 5/2$, the expression coincides with the one predicted by the heterogeneous mean-field (HMF) theory [43] (see Appendix H), while HMF theory is violated for $\gamma > 5/2$. In LPA networks, Λ_M is, for any γ, given by $\sqrt{q_{max}}$, so Eq. (6) predicts a vanishing of the epidemic threshold qualitatively different from the one on uncorrelated networks for $\gamma < 5/2$. In particular, the approach to zero in the thermodynamic limit should be *slower* in LPA networks than in static uncorrelated networks with the same γ.
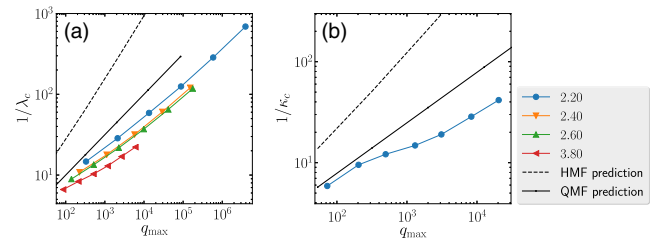

FIG. 5.   (a) Numerical estimate of the inverse epidemic threshold $1/\lambda_c$ in LPA as a function of q_{max}, for various values of the exponent γ. We consider networks of sizes from $N = 10^2$ to $N = 10^8$. (b) Numerical estimate of the synchronization threshold κ_c for $\gamma = 2.2$ as a function of q_{max}. System size ranges from $N = 300$ to $N = 300\,000$. In both plots the dependence for $\gamma = 2.2$ predicted by the QMF theory is represented by a thick dashed straight line, and the HMF prediction is represented by a dash-dotted line.

FIG. 4.   (a) Largest eigenvalue Λ_M as a function of $\sqrt{q_{max}}$ in rewired LPA networks with different degree exponent γ. (b) Inverse participation ratio $Y_4(N)$ as a function of N in rewired LPA networks with different degree exponent γ. Each point in both graphs corresponds to an average over 100 independent network realizations. Error bars are smaller than symbol sizes.

In order to check this picture, we perform numerical simulations of the SIS model on LPA networks of different degree exponent γ and determine the threshold using the lifespan method (see Appendix H). In Fig. 5(a), we plot the numerically estimated threshold as a function of q_{max}. We find that the theoretical expectation is followed only approximately: The slopes are smaller than 1 in all cases, more so for larger values of γ. However, this discrepancy is a finite-size effect: As the system size grows, the effective slope grows. Asymptotically, for large N, the threshold always vanishes as $\sqrt{q_{max}}$, at variance with what happens for uncorrelated static networks for $\gamma < 5/2$. The comparison with the slope predicted by HMF theory for $\gamma = 2.2$ (dashed line) clearly shows the failure of the latter. Hence, the remarkable conclusion is that on LPA networks, the epidemic threshold vanishes asymptotically for any γ, but it never vanishes as predicted by HMF theory, at odds with what happens on static uncorrelated networks.

In the case of real-world networks, our proposed estimate for the scaling of the largest eigenvalue again provides a much better overall prediction for the threshold in the SIS model—see Fig. 6, where we compare it with the original CLV prediction. As we can see, in cases where the CLV prediction is off by orders of magnitude, our improved scaling form leads to a much better threshold prediction. As an estimate of the overall goodness of the prediction, the mean relative error for the CLV predictions is 4.20 (standard deviation 11.92, maximum 52.02), while the predictions of Eq. (4) give much smaller values (mean 0.37, standard deviation 0.24, maximum 1.33).
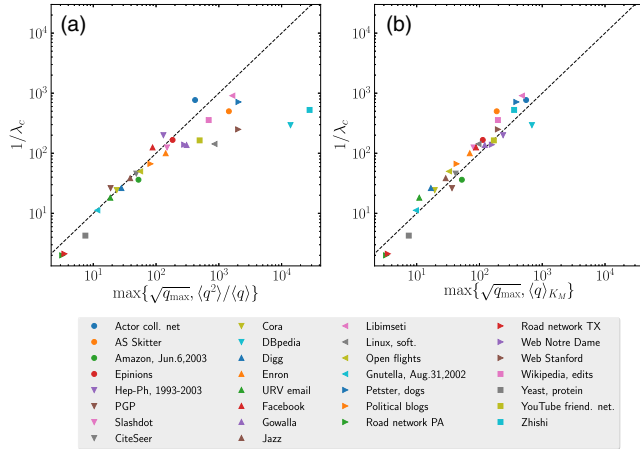

FIG. 6.   (a) Numerical estimate of the inverse epidemic threshold $1/\lambda_c$, in a subset of the real-world networks considered, as a function of the inverse largest eigenvalue approximation $\max\{\sqrt{q_{max}}, \langle q^2 \rangle / \langle q \rangle\}$. (b) Numerical estimate of the inverse epidemic threshold $1/\lambda_c$ in real-world networks as a function of the inverse improved largest eigenvalue approximation $\max\{\sqrt{q_{max}}, \langle q \rangle_{K_M}\}$. Data for the networks Zhishi, Web Notre Dame, Road network TX, and Road network PA are lower bounds to the real threshold due to computing-time limitations.

B. Synchronization

Kuramoto dynamics [44] (see Appendix I) is the paradigmatic model for the study of synchronization among weakly coupled oscillators, with applications ranging from neural networks to charge-density waves. Its behavior in networks has been investigated in great detail [45,46], showing the existence of a synchronization threshold for a coupling parameter, κ_c, separating a random phase from a synchronized phase. Concerning the synchronization threshold, the standard approach is the one in Ref. [8], predicting a synchronized state to appear when the coupling κ among oscillators is larger than the critical value,

$$\kappa_c = \frac{k_0}{\Lambda_M}, \tag{7}$$

where $k_0 = 2/[\pi g(0)]$ and $g(\omega)$ is the frequency distribution of individual oscillators (see Appendix I). To assess whether the generalized scaling just uncovered for Λ_M on LPA networks also has effects for these dynamics, we perform simulations of the Kuramoto model on growing networks and determine the critical coupling κ_c (see Appendix I for details).

Figure 5(b) clearly shows that also for these dynamics, the prediction given by the inverse of the LEV is qualitatively correct and, as a consequence, for $\gamma < 5/2$, the threshold vanishes more slowly than what is predicted for random uncorrelated networks. We conclude that also in this case, the nature of the growing network, and, in particular, the lack of a K-core structure, has profound consequences for the dynamics mediated by the contact network.

VI. DISCUSSION

The generalized CLV conjecture we have exposed allows us to fully clarify the physical origin of the properties of the adjacency matrix's largest eigenpair in complex networks. There are two subgraphs that determine the LEV and the PEV in a large complex network: the hub with its spokes and the densely mutually interconnected set of nodes singled out as the maximum K-core [47]. Each of these two subgraphs has (in isolation) an associated LEV: The hub is the center of a star graph, and therefore $\Lambda_M^{(h)} = \sqrt{q_{max}}$; the maximum K-core is a homogeneous graph, and therefore $\Lambda_M^{(K_M)} \simeq \langle q \rangle_{K_M}$. The LEV of the global topology is simply given by the largest of the two. In uncorrelated static networks, the growth with N of the two individual LEVs depends on γ, and this gives rise to the change of behavior occurring for $\gamma = 5/2$, Eq. (3). In growing LPA networks, the K-core structure is, by construction, absent: The spectral properties are dictated only by the hub (and this remains true also after reshuffling). In networks of any origin (and any correlation level), the relation between the average degree of the max K-core and

$\langle q^2 \rangle / \langle q \rangle$ may break down. However, it is still true that the LEV value is the largest between $\Lambda_M^{(h)}$ and $\Lambda_M^{(K_M)}$.

This conjecture is clearly not a proof. However, the understanding of its conceptual origin allows us to predict that it should hold for practically all real-world networks. Various different mechanisms may lead to its breakdown. There could be an inhomogeneous max K-core in the network such that $\Lambda_M^{(K_M)}$ is very different from $\langle q \rangle_{K_M}$. There could be a third, different, type of subgraph, characterized by a LEV larger than both the others. Or the whole graph could have a LEV larger than the LEV of any proper subgraph. An example of this last case is the complete bipartite network $K_{p,q}$: Its LEV is $\sqrt{pq}$ [1], which can be much larger (assuming $p \leq q$) than the value $\max\{\sqrt{q}, p\}$ predicted by Eq. (4). All these mechanisms are, in principle, possible; however, they appear to be unlikely in real self-organized networks.

Our findings about spectral properties have immediate implications in several contexts. We have shown that properties of dynamical processes as general as epidemics and synchronization are deeply affected by which subgraph determines the LEV. For example, another effect that can be immediately predicted is that removing the hub may completely disrupt the dynamics when the LEV is given by $\Lambda_M^{(h)}$, while this is practically inconsequential in the other case. Similar consequences are expected to occur in general [9–11,41]. Another context where these results may have implications is for centrality measures, many of which are variations of the eigenvalue centrality [6,48]. Finally, it is worth remarking that the example of linear preferential attachment networks clearly points out that the way a network is built may have deep and unexpected implications for its structure and its functionality.

ACKNOWLEDGMENTS

APPENDIX A: APPLICABILITY OF CLV EXACT RESULTS TO FINITE NETWORKS

The exact result proved by Chung, Lu, and Vu in Ref. [17], namely, Eq. (1), can be rewritten as

$$\Lambda_M = \begin{cases} a_1 \sqrt{q_{\max}} & \text{if } \frac{\langle q^2 \rangle}{\langle q \rangle \sqrt{q_{\max}}} < \frac{1}{\ln^2(N)} \\ a_2 \frac{\langle q^2 \rangle}{\langle q \rangle} & \text{if } \frac{\langle q^2 \rangle}{\langle q \rangle \sqrt{q_{\max}}} > \ln(N). \end{cases} \quad \text{(A1)}$$

It therefore provides a prediction for the value of the LEV if the ratio

$$\zeta(\gamma, N) \equiv \frac{\langle q^2 \rangle}{\langle q \rangle \sqrt{q_{\max}}} \quad \text{(A2)}$$

is larger than $\ln(N)$ or smaller than $1/\ln^2(N)$. For very large systems, both $\langle q^2 \rangle / \langle q \rangle$ and $\sqrt{q_{\max}}$ diverge and, if they scale with N with different exponents (i.e., $\gamma \neq 5/2$), the logarithmic factors are not asymptotically relevant: Either the first or the second of the conditions in Eq. (1) is fulfilled. However, for finite values of N, there is a sizable interval such that Eq. (1) does not strictly apply. In the case of uncorrelated power-law networks with distribution $P(q) = (\gamma - 1)m^{\gamma-1}q^{-\gamma}$, we have, in the continuous degree approximation,

$$\zeta(\gamma, N) = \frac{\gamma - 2}{3 - \gamma} \frac{m}{\sqrt{q_{\max}}} \left[\left(\frac{q_{\max}}{m} \right)^{3-\gamma} - 1 \right], \quad \text{(A3)}$$

where $q_{\max} = N^{1/2}$ for $\gamma < 3$ and $q_{\max} = N^{1/(\gamma-1)}$ for $\gamma > 3$, m is the minimum degree, for which we take $m = 3$, and in the evaluation of $\langle q^2 \rangle$, we have taken the maximum degree $q_{\max}$ into account. Numerically evaluating $\zeta(\gamma, N)$, we can compute, for every value of γ, the minimum value of N for the exact expression Eq. (1) to apply. For $\gamma < 5/2$, $\zeta(\gamma, N)$ diverges with N: The prediction $\Lambda_M \approx \langle q^2 \rangle / \langle q \rangle$ in Eq. (1) applies for $N > N_{\min}$ defined by $\zeta(\gamma, N_{\min}) = \ln(N_{\min})$. On the other hand, for $\gamma > 5/2$, $\zeta(\gamma, N)$ tends to zero as the system size diverges. Hence, the prediction $\Lambda_M \approx \sqrt{q_{\max}}$ in Eq. (1) applies for $N > N_{\min}$, defined in this case by $\zeta(\gamma, N_{\min}) = 1/\ln^2(N_{\min})$. In Fig. 7, we plot $N_{\min}$ as a function of γ. From the figure, it turns out that the exact theoretical prediction Eq. (1) holds only for extremely large sizes (at least $N > 10^{11}$, but the bound is much larger for almost all values of γ). Networks of such size cannot be simulated with current computer resources. An improved analysis in Ref. [17] replaces $\ln(N)$ by $\ln(N)^{1/2}$ and $\ln(N)^2$ by $\ln(N)^{3/2}$ in Eq. (1). A similar analysis as performed above indicates that this corrected version holds for sizes of at least $N > 3 \times 10^7$, which is
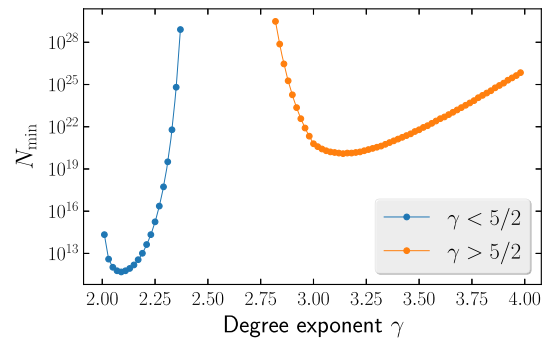

FIG. 7. Minimum sizes $N_{\min}$ for the validity of Eq. (1) in uncorrelated power-law networks as a function of the degree exponent γ. Values in the vicinity of $\gamma = 5/2$ not plotted are all larger than 10^{30}.
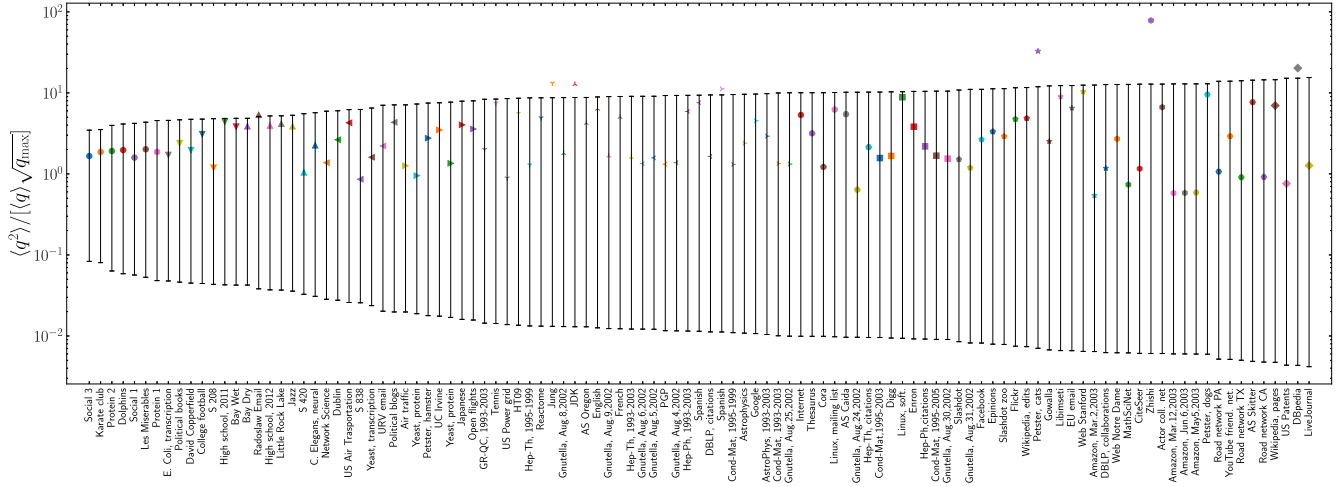
FIG. 8.   For each of the real-world networks considered, we plot in log scale a line indicating the interval where Eq. (1) does not make any prediction. The symbols indicate the actual value of $\langle q^2 \rangle / [\langle q \rangle \sqrt{q_{max}}]$ for each network.

very close to the limit allowed by present computation systems.

In the case of the real-world networks considered, we plot in Fig. 8, along the y axis, a line between $\ln(N)$ and $1/\ln^2(N)$, indicating the interval of values of $\langle q^2 \rangle / [\langle q \rangle \sqrt{q_{max}}]$ where Eq. (1) does not strictly apply. The symbols indicate the actual value of the ratio $\langle q^2 \rangle / [\langle q \rangle \sqrt{q_{max}}]$ in each network. It turns out that for 102 networks out of 109, the actual value falls in the inapplicability interval. Hence, for the vast majority of real networks, the exact result in Eq. (1) does not, strictly speaking, allow us to make any prediction.

APPENDIX B: EIGENVECTOR LOCALIZATION AND THE INVERSE PARTICIPATION RATIO

The concept of the localization of the principal eigenvector $\{f_i\}$ translates in determining whether the value of its normalized components (satisfying $\sum_i f_i^2 = 1$) is evenly distributed among all nodes in the network or it attains a large value on some subset of nodes V and is much smaller in all the rest. In the first case $f_i \sim N^{-1/2}$, $\forall i$ and the network is not localized. In the second case $f_i \sim N_V^{-1/2}$, for $i \in V$ and $f_i \sim 0$, for $i \notin V$, were N_V is the size of the localization subset V.

The presence of localization in the PEV can be easily assessed in ensembles of networks of variable size N by studying the inverse participation ratio (IPR), defined as [30,31]

$$Y_4(N) = \sum_{i=1}^{N} [f_i]^4, \tag{B1}$$

as a function of N, and fitting its behavior to a power-law decay of the form [27]

$$Y_4(N) \sim N^{-\alpha}. \tag{B2}$$

If the PEV is delocalized, with $f_i \sim N^{-1/2}$, $\forall i$, the exponent α is equal to 1. Any exponent $\alpha < 1$ indicates the presence of some form of eigenvector localization, taking place in a subextensive set of nodes, of size $N_V \sim N^\alpha$. In the extreme case of localization on a single node, or a set of nodes with fixed size, we have $\alpha = 0$ and $Y_4(N) \sim$ const.

APPENDIX C: K-CORE DECOMPOSITION

The K-core decomposition [28] is an iterative procedure to classify vertices of a network in layers of increasing density of mutual connections. Starting with the whole graph, one removes the vertices with only one connection (degree $q = 1$). This procedure is then repeated until only nodes with degree $q \geq 2$ are left. The removed nodes constitute the $K = 1$ shell, and those remaining are the $K = 2$ core. At the next step, all vertices with degree $q = 2$ are removed, thus leaving the $K = 3$ core. The procedure is repeated iteratively. The maximum K-core (of index K_M) is the set of vertices such that one more iteration of the procedure removes all of them. Notice that all vertices of the K-core of index K have degree larger than or equal to K.

APPENDIX D: DIFFERENT LOCALIZATIONS FOR UCM NETWORKS

For UCM networks, the localization of the PEV in different subgraphs depending on whether γ is larger or smaller than $5/2$ can be exposed by plotting the weights concentrated on the subgraphs as a function of γ (see Fig. 9). In this figure, we have set the weight of the maximum K-core equal to zero for $\gamma = 3$ since, by construction, it coincides with the whole network and trivially contains all the weight for the PEV.

It is clear that for $\gamma < 5/2$, the weight is concentrated on the max K-core, while the hub plays no role. For $\gamma > 5/2$, the opposite scenario applies: The hub plus its nearest
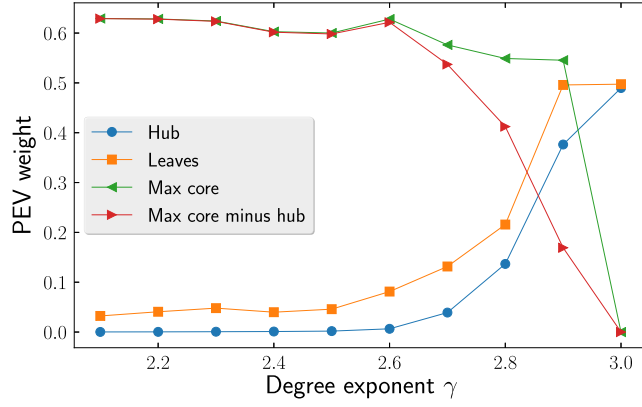
FIG. 9.   PEV weight concentrated on various subgraphs for UCM networks of size $N = 10^7$ with different values of γ.

neighbors (i.e., the leaves) bear most of the PEV weight, while the max K-core (or the max K-core minus the hub, in case the latter belongs to the former) has vanishing weight concentrated on it. Strong finite-size effects smoothen the change of behavior for γ between $5/2$ and 3, but by changing the system size (not shown), one can extrapolate that, for asymptotically large systems, the picture is the one just described.

APPENDIX E: BUILDING LINEAR PREFERENTIAL ATTACHMENT NETWORKS

Given the mapping of LPA networks with the Price model [49], LPA networks can be easily constructed with the following simplified algorithm [5]: Every time step, a new node is added, with m new edges. Each one of them is connected to an old node, chosen uniformly at random, with probability $\phi = a/(a + m)$; otherwise, with the complementary probability $1 - \phi = m/(a + m)$, the edge is connected to a node chosen with probability proportional to its in-degree $q_s(t) - m$. In our simulations, we consider LPA networks with minimum degree $m = 2$ and varying γ, for network sizes ranging from $N = 10^2$ up to $N = 10^8$. Topological and spectral properties of LPA networks are computed by averaging over 100 different network configurations for each value of γ and N.

APPENDIX F: PRINCIPAL EIGENVECTOR LOCALIZATION IN LINEAR PREFERENTIAL ATTACHMENT NETWORKS

A direct way to observe PEV localization consists in plotting the square of the components f_i^2 as a function of the node degree q_i, as shown in Fig. 10. As we can see from this figure, for all values of γ, the component of the PEV associated with the largest values of q have a macroscopic weight, indicating localization of the PEV in the hubs. This plot presents evidence of a further difference of LPA networks with respect to random uncorrelated networks. In this case, and for $\gamma < 5/2$, it is possible to show that in
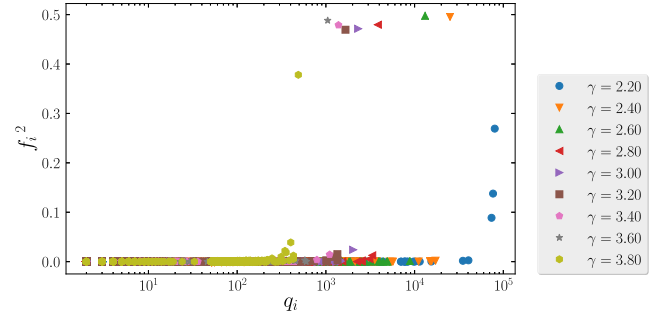

FIG. 10.   Scatter plot of f_i^2 as a function of the degree q_i in LPA networks of different degree exponent γ. Network size $N = 10^6$.

static networks, the PEV components approach the form obtained within the annealed network approximation [50], which is given by [27]

$$f_i^{an} = \frac{q_i}{[N\langle q^2\rangle]^{1/2}}. \tag{F1}$$

As we can see in Fig. 10, this linear behavior is not present in the data from LPA networks, even for small γ values.

APPENDIX G: K-CORE STRUCTURE IN RESHUFFLED LINEAR PREFERENTIAL ATTACHMENT NETWORKS

The lack of K-core structure of LPA networks arises from its peculiar growing nature, in which nodes with minimum degree m are sequentially attached to the network. This property is not robust, however, since a simple reshuffling procedure can destroy it, inducing a nontrivial K-core structure. In Fig. 11, we show the average maximum core index $\langle K_M\rangle$ as a function of the network size, computed from LPA networks with different degree exponent, in which edges have been reshuffled according to the degree-preserving edge-rewiring process described in Ref. [40]. As we can observe, for $\gamma \geq 3$, the reshuffling process is not able to induce a substantial K-core structure. This occurs because the reshuffling destroys correlations, but uncorrelated networks with $\gamma > 3$ have essentially no
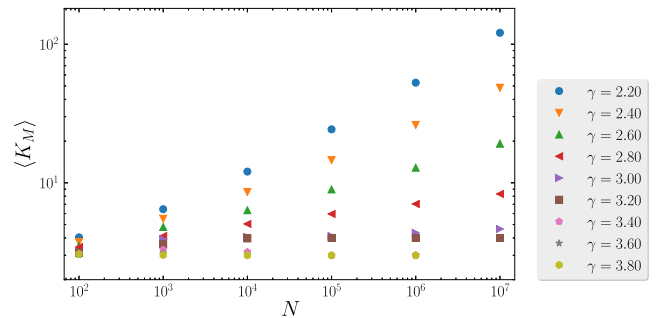

FIG. 11.   Average maximum core index $\langle K_M\rangle$ as a function of network size for reshuffled LPA networks with different degree exponent γ. Error bars are smaller than symbol sizes.

FIG. 12.   Average maximum core index $\langle K_M \rangle$ as a function of network size for reshuffled LPA networks with different degree exponent γ. Error bars are smaller than symbol sizes.
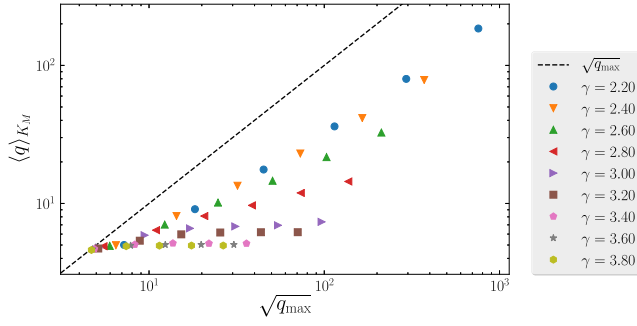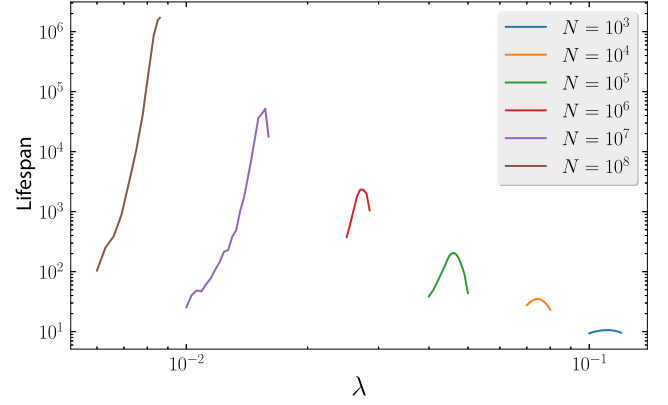

FIG. 13.   Average lifespan vs spreading rate λ_c of SIS epidemics starting from a single infected node (the hub) and reaching the healthy absorbing state before the coverage reaches the threshold value $c = 0.5$. Data are for LPA networks with $\gamma = 2.6$ and various system size N.

K-core structure [29]. For $\gamma < 3$, on the other hand, the K-core structure generated by reshuffling is robust, with an average maximum core index increasing as a power law with network size [29].

The maximum K-core resulting from the reshuffling of LPA networks has an average degree $\langle q \rangle_{K_M}$ that depends on the maximum degree q_{max} (see Fig. 12). However, since the hub has degree much larger than $N^{1/2}$, the network does not become uncorrelated even upon randomization, and $\langle q \rangle_{K_M}$ is always smaller than $\sqrt{q_{max}}$. Hence, the properties of the largest eigenpair are always dictated by the hub, as in the original LPA networks.

APPENDIX H: SUSCEPTIBLE-INFECTED-SUSCEPTIBLE EPIDEMIC DYNAMICS

The SIS model is the simplest model designed to capture the properties of diseases that do not confer immunity [51]. In the SIS model, individuals can be in either of two states, susceptible or infected. Susceptible individuals become infected through contact with an infected individual at rate β, while infected individuals heal spontaneously at rate μ. As a function of the parameter $\lambda = \beta/\mu$, the model shows a nonequilibrium phase transition between an active, infected phase for $\lambda > \lambda_c$ and an inactive, healthy phase for $\lambda \leq \lambda_c$. We are interested in the location of the so-called epidemic threshold λ_c and on its dependence on the topological properties of the network under consideration [52].

Early theoretical approaches to the SIS dynamics were based on the so-called heterogeneous mean-field (HMF) theory [43,53], which neglects both dynamical and topological correlations by replacing the actual structure of the network, as given by the adjacency matrix, by an annealed version in which edges are constantly rewired, while preserving the degree distribution $P(q)$. Within this annealed network approximation [54], a threshold for uncorrelated networks of the form $\lambda_c = \langle q \rangle / \langle q^2 \rangle$ is obtained. An improvement over this approximate theory is given by quenched mean-field (QMF) theory [7], which, while still neglecting dynamical correlations, takes into

account the full structure of the adjacency matrix. Within this approximation, the threshold is given by the inverse of the largest eigenvalue of the adjacency matrix, $\lambda_c = 1/\Lambda_M$. Recent and intense activity, based on more sophisticated approaches [22,55,56], has shown that, on uncorrelated static networks, this result is essentially asymptotically correct.

In order to determine λ_c numerically, we resort to the lifespan method [56,57], which is not affected by the drawbacks that make the consideration of susceptibility unwieldy [55]. Simulations start with only the hub infected. For each run, one keeps track of the coverage, i.e., the fraction of different nodes that have been touched at least once by the infection. In an infinite network, this quantity is vanishing for $\lambda \leq \lambda_c$, while it tends asymptotically to 1 in the active region of the phase diagram. In finite networks, one can set a threshold c (we choose $c = 0.5$) and consider all runs that reach a coverage larger than c as endemic. The average lifespan $\langle T \rangle$, restricted only to nonendemic runs, plays the role of a susceptibility: The position of the threshold is estimated as the value of λ for which $\langle T \rangle$ reaches a peak (see Fig. 13).

APPENDIX I: KURAMOTO SYNCHRONIZATION DYNAMICS

The Kuramoto model [44,46] describes the dynamics of a collection of weakly coupled, nearly identical oscillators. If they are placed on the nodes of a network with adjacency matrix A_{ij}, the equation of motion reads

$$\dot{\theta}_i = \omega_i + \kappa \sum_j A_{ij} \sin(\theta_j - \theta_i), \qquad (I1)$$

where κ is a coupling constant and ω_i is a quenched random variable (natural frequency), whose distribution $g(\omega)$ is taken here to be uniform between -1 and 1. In the initial

condition, the phases θ_i are uniformly random between 0 and 2π. Defining the global order parameter as

$$r = \left| \frac{1}{N} \sum_i e^{-I\theta_i} \right|, \tag{I2}$$

where I is the imaginary unit, one finds that there is a critical threshold κ_c separating a disordered phase where $r = 0$ (in the thermodynamic limit) from a synchronized phase with $r > 0$. A QMF-like theory for the Kuramoto model [8] predicts a critical point $\kappa_c = k_0/\Lambda_M$, where $k_0 = 2/[\pi g(0)] = 4/\pi$, the last equality holding because of the uniform distribution of natural frequencies $g(\omega)$.

The value of the critical threshold is numerically determined in finite networks by computing the susceptibility, $\chi_K(\kappa) = N(\langle r^2 \rangle - \langle r \rangle^2)$, which shows a peak for $\kappa = \kappa_c$.

———

[1] P. Van Mieghem, *Graph Spectra for Complex Networks* (Cambridge University Press, Cambridge, England, 2011).

[2] A. N. Samukhin, S. N. Dorogovtsev, and J. F. F. Mendes, *Laplacian Spectra of, and Random Walks on, Complex Networks: Are Scale-Free Architectures Really Important?*, Phys. Rev. E **77**, 036115 (2008).

[3] S. Fortunato, *Community Detection in Graphs*, Phys. Rep. **486**, 75 (2010).

[4] B. Karrer, M. E. J. Newman, and L. Zdeborová, *Percolation on Sparse Networks*, Phys. Rev. Lett. **113**, 208702 (2014).

[5] M. Newman, *Networks: An Introduction* (Oxford University Press, New York, 2010).

[6] P. Bonacich, *Factoring and Weighting Approaches to Status Scores and Clique Identification*, J. Math. Sociol. **2**, 113 (1972).

[7] D. Chakrabarti, Y. Wang, C. Wang, J. Leskovec, and C. Faloutsos, *Epidemic Thresholds in Real Networks*, ACM Trans. Inform. Syst. Sec. **10**, 13 (2008).

[8] J. G. Restrepo, E. Ott, and B. R. Hunt, *Onset of Synchronization in Large Networks of Coupled Oscillators*, Phys. Rev. E **71**, 036151 (2005).

[9] J. G. Restrepo, E. Ott, and B. R. Hunt, *Weighted Percolation on Directed Networks*, Phys. Rev. Lett. **100**, 058701 (2008).

[10] A. Pomerance, E. Ott, M. Girvan, and W. Losert, *The Effect of Network Topology on the Stability of Discrete State Models of Genetic Control*, Proc. Natl. Acad. Sci. U.S.A. **106**, 8209 (2009).

[11] O. Kinouchi and M. Copelli, *Optimal Dynamical Range of Excitable Networks at Criticality*, Nat. Phys. **2**, 348 (2006).

[12] S. N. Dorogovtsev, A. V. Goltsev, J. F. F. Mendes, and A. N. Samukhin, *Spectra of Complex Networks*, Phys. Rev. E **68**, 046109 (2003).

[13] D.-H. Kim and A. E. Motter, *Ensemble Averageability in Network Spectra*, Phys. Rev. Lett. **98**, 248701 (2007).

[14] R. R. Nadakuditi and M. Newman, *Spectra of Random Graphs with Arbitrary Expected Degrees*, Phys. Rev. E **87**, 012803 (2013).

[15] J. G. Restrepo, E. Ott, and B. R. Hunt, *Approximating the Largest Eigenvalue of Network Adjacency Matrices*, Phys. Rev. E **76**, 056119 (2007).

[16] A.-L. Barabási and R. Albert, *Emergence of Scaling in Random Networks*, Science **286**, 509 (1999).

[17] F. Chung, L. Lu, and V. Vu, *Spectra of Random Graphs with Given Expected Degrees*, Proc. Natl. Acad. Sci. U.S.A. **100**, 6313 (2003).

[18] M. Boguñá, R. Pastor-Satorras, and A. Vespignani, *Cut-offs and Finite Size Effects in Scale-Free Networks*, Eur. Phys. J. B **38**, 205 (2004).

[19] M. Boguñá and R. Pastor-Satorras, *Class of Correlated Random Networks with Hidden Variables*, Phys. Rev. E **68**, 036112 (2003).

[20] F. Chung, L. Lu, and V. Vu, *Eigenvalues of Random Power Law Graphs*, Ann. Comb. **7**, 21 (2003).

[21] S. N. Dorogovtsev and J. F. F. Mendes, *Evolution of Networks*, Adv. Phys. **51**, 1079 (2002).

[22] C. Castellano and R. Pastor-Satorras, *Thresholds for Epidemic Spreading in Networks*, Phys. Rev. Lett. **105**, 218701 (2010).

[23] G. H. Golub and C. F. Van Loan, *Matrix Computations* (JHU Press, Baltimore, 2012), Vol. 3.

[24] M. Catanzaro, M. Boguñá, and R. Pastor-Satorras, *Generation of Uncorrelated Random Scale-Free Networks*, Phys. Rev. E **71**, 027103 (2005).

[25] F. Radicchi and C. Castellano, *Breaking of the Site-Bond Percolation Universality in Networks*, Nat. Commun. **6**, 10196 (2015).

[26] C. Castellano and R. Pastor-Satorras, *Competing Activation Mechanisms in Epidemics on Networks*, Sci. Rep. **2**, 371 (2012).

[27] R. Pastor-Satorras and C. Castellano, *Distinct Types of Eigenvector Localization in Networks*, Sci. Rep. **6**, 18847 (2016).

[28] S. B. Seidman, *Network Structure and Minimum Degree*, Soc. Networks **5**, 269 (1983).

[29] S. N. Dorogovtsev, A. V. Goltsev, and J. F. F. Mendes, *K-Core Organization of Complex Networks*, Phys. Rev. Lett. **96**, 040601 (2006).

[30] A. V. Goltsev, S. N. Dorogovtsev, J. G. Oliveira, and J. F. F. Mendes, *Localization and Spreading of Diseases in Complex Networks*, Phys. Rev. Lett. **109**, 128702 (2012).

[31] T. Martin, X. Zhang, and M. E. J. Newman, *Localization and Centrality in Networks*, Phys. Rev. E **90**, 052808 (2014).

[32] See Supplemental Material at http://link.aps.org/supplemental/10.1103/PhysRevX.7.041024 for a table describing the topological properties of the real networks considered.

[33] S. Bhamidi, S. N. Evans, and A. Sen, *Spectra of Large Random Trees*, J. Theor. Probab. **25**, 613 (2012).

[34] M. Krivelevich and B. Sudakov, *The Largest Eigenvalue of Sparse Random Graphs*, Comb. Probab. Comput. **12**, 61 (2003).

[35] S. N. Dorogovtsev, J. F. F. Mendes, and A. N. Samukhin, *Structure of Growing Networks with Preferential Linking*, Phys. Rev. Lett. **85**, 4633 (2000).

[36] A. Barrat and R. Pastor-Satorras, *Rate Equation Approach for Correlations in Growing Network Models*, Phys. Rev. E **71**, 036127 (2005).

[37] M. E. J. Newman, *Assortative Mixing in Networks*, Phys. Rev. Lett. **89**, 208701 (2002).

[38] R. Pastor-Satorras, A. Vázquez, and A. Vespignani, *Dynamical and Correlation Properties of the Internet*, Phys. Rev. Lett. **87**, 258701 (2001).

[39] A. Flaxman, A. Frieze, and T. Fenner, *High Degree Vertices and Eigenvalues in the Preferential Attachment Graph*, Internet Math. **2**, 1 (2005).

[40] S. Maslov and K. Sneppen, *Specificity and Stability in Topology of Protein Networks*, Science **296**, 910 (2002).

[41] D. B. Larremore, W. L. Shew, and J. G. Restrepo, *Predicting Criticality and Dynamic Range in Complex Networks: Effects of Topology*, Phys. Rev. Lett. **106**, 058101 (2011).

[42] R. M. Anderson and R. M. May, *Infectious Diseases in Humans* (Oxford University Press, Oxford, 1992).

[43] R. Pastor-Satorras and A. Vespignani, *Epidemic Spreading in Scale-Free Networks*, Phys. Rev. Lett. **86**, 3200 (2001).

[44] J. A. Acebrón, L. L. Bonilla, C. J. Pérez Vicente, F. Ritort, and R. Spigler, *The Kuramoto Model: A Simple Paradigm for Synchronization Phenomena*, Rev. Mod. Phys. **77**, 137 (2005).

[45] A. Arenas, A. Díaz-Guilera, J. Kurths, Y. Moreno, and C. Zhou, *Synchronization in Complex Networks*, Phys. Rep. **469**, 93 (2008).

[46] F. A. Rodrigues, T. K. DM. Peron, P. Ji, and J. Kurths, *The Kuramoto Model in Complex Networks*, Phys. Rep. **610**, 1 (2016).

[47] Notice that, in many cases, the hub is actually part of the maximum K-core. Nevertheless, there is a clear distinction between the case in which the PEV is localized on the hub and its immediate neighbors or the PEV is localized around the maximum K-core as a whole.

[48] L. Katz, *A New Status Index Derived from Sociometric Analysis*, Psychometrika **18**, 39 (1953).

[49] D. J. de Solla Price, *A General Theory of Bibliometric and Other Cumulative Advantage Processes*, J. Am. Soc. Inf. Sci. **27**, 292 (1976).

[50] M. Boguñá, C. Castellano, and R. Pastor-Satorras, *Langevin Approach for the Dynamics of the Contact Process on Annealed Scale-Free Networks.*, Phys. Rev. E **79**, 036110 (2009).

[51] M. J. Keeling and P. Rohani, *Modeling Infectious Diseases in Humans and Animals* (Princeton University Press, Princeton, NJ, 2007).

[52] R. Pastor-Satorras, C. Castellano, P. Van Mieghem, and A. Vespignani, *Epidemic Processes in Complex Networks*, Rev. Mod. Phys. **87**, 925 (2015).

[53] R. Pastor-Satorras and A. Vespignani, *Epidemic Dynamics and Endemic States in Complex Networks*, Phys. Rev. E **63**, 066117 (2001).

[54] S. N. Dorogovtsev, A. V. Goltsev, and J. F. F. Mendes, *Critical Phenomena in Complex Networks*, Rev. Mod. Phys. **80**, 1275 (2008).

[55] S. C. Ferreira, C. Castellano, and R. Pastor-Satorras, *Epidemic Thresholds of the Susceptible-Infected-Susceptible Model on Networks: A Comparison of Numerical and Theoretical Results*, Phys. Rev. E **86**, 041125 (2012).

[56] M. Boguñá, C. Castellano, and R. Pastor-Satorras, *Nature of the Epidemic Threshold for the Susceptible-Infected-Susceptible Dynamics in Networks*, Phys. Rev. Lett. **111**, 068701 (2013).

[57] A. S. Mata, M. Boguñá, C. Castellano, and R. Pastor-Satorras, *Lifespan Method as a Tool to Study Criticality in Absorbing-State Phase Transitions*, Phys. Rev. E **91**, 052117 (2015).